

Figure 1. Perspective view of the complex cation of **1** ($[\text{Ni}\{\text{Co}(\text{aet})_2(\text{en})\}_2]^{4+}$) with the atomic labeling scheme. Unlabeled atoms are related to labeled atoms by the 2-fold axis through the Co1, Ni, and Co2 atoms. Ellipsoids represent 50% probability.

resolving agent, showing CD extrema with opposite signs at 516 and 463 nm. All the aet and en chelate rings possess a distinct gauche form with the λ conformation for the $\Delta\Delta$ isomer and the δ one for the $\Lambda\Lambda$ isomer, and furthermore all four bridging sulfur atoms are fixed to the *S* configuration for the $\Delta\Delta$ isomer and the *R* one for the $\Lambda\Lambda$ isomer. The ^{13}C NMR spectrum of **1** in D_2O gives only two signals due to methylene carbons of the four aet ligands and one signal due to methylene carbons of the two en ligands.⁵ In the 500-MHz ^1H NMR spectrum methylene protons of the four aet ligands appear as two sets of doublets and two sets of triplets and those of the two en ligands appear as two sets of doublets.⁵ These NMR spectral behavior demonstrate that the geometry around the two $\text{C}_2\text{-cis}(\text{S})\text{-}[\text{Co}(\text{aet})_2(\text{en})]^+$ subunits observed in the crystal is retained in solution, having a D_2 symmetrical structure.

The electronic absorption spectrum of **1** in water⁵ is characterized by the three intense absorption bands at 27.78×10^3 , 37.31×10^3 , and $42.02 \times 10^3 \text{ cm}^{-1}$. Treatment of **1** (0.1 g) with 10% H_2O_2 (2.5 cm^3) in water, followed by the addition of 15% HBr (1 cm^3), led the solution color change from red-brown to yellow, from which the yellow complex (**2**) was isolated in 81% yield.⁹ The absorption spectrum of **2** is quite similar to those of *cis*-(*S*)- $[\text{Co}(\text{sulfinato-}S)_2(\text{amine})_4]^+$ type complexes over the whole region.¹⁰ In the ^{13}C NMR spectrum **2** gives two sharp signals at δ 40.83 and 64.16 and a signal which splits into two at δ 46.57 and 46.68.⁹ From these facts and elemental analysis, **2** can be confidently assigned the $\text{C}_2\text{-cis}(\text{S})\text{-}[\text{Co}(\text{NH}_2\text{CH}_2\text{CH}_2\text{SO}_2\text{-}N\text{-}S)_2(\text{en})]\text{Br}$ formula; that is, the H_2O_2 oxidation of **1** causes the cleavage of Ni–S bonds to form the mononuclear sulfinato Co(III) complex, retaining the $\text{C}_2\text{-cis}(\text{S})$ geometry of the $[\text{Co}(\text{aet})_2(\text{en})]^+$ subunits.

In the present work, the reaction of $[\text{Ni}(\text{aet})_2]$ and $[\text{CoCl}_2(\text{en})_2]^+$ under a moderate condition gave the S-bridged $\text{Co}^{\text{III}}\text{-Ni}^{\text{II}}\text{Co}^{\text{III}}$ complex **1** containing $\text{C}_2\text{-cis}(\text{S})\text{-}[\text{Co}(\text{aet})_2(\text{en})]^+$ subunits, and furthermore the mononuclear sulfinato complex **2** was derived from **1** with retention of the $\text{C}_2\text{-cis}(\text{S})$ geometry. This result obviously implies that the bidentate-*N,S* ligand aet readily transfers from Ni(II) to Co(III) coordination sphere. It is noted that the mononuclear $[\text{Co}(\text{aet})_2(\text{en})]^+$ has not been prepared to date; the direct reaction of Co^{2+} , 2-aminoethanethiol, cystamine, and ethylenediamine results in the formation of $[\text{Co}(\text{aet})(\text{en})_2]^{2+}$, $[\text{Co}(\text{aet})_3]$, and $[\text{Co}_2(\text{aet})_3]^{2+}$.¹¹ In addition, the analogous

$[\text{Co}(\text{L-cys-}N,S)_2(\text{en})]^-$, which is formed by the reaction of Co^{2+} , L-cysteine, L-cystine, and ethylenediamine, is not stable enough to be isolated, converting into polymeric structures in water.^{11,12} Taking these facts into consideration, it is assumed that the *cis*-(*S*)- $[\text{Co}(\text{aet})_2(\text{en})]$ arrangement in $[\text{Ni}\{\text{Co}(\text{aet})_2(\text{en})\}_2]^{4+}$ is stabilized by the S-bridged structure with the central Ni(II).

Supplementary Material Available: Tables A–C, listing atomic coordinates and equivalent isotropic thermal parameters, bond distances and angles, and anisotropic thermal parameters for **1** (3 pages); Table D, listing observed and calculated structure factors for **1** (11 pages). Ordering information is given on any current masthead page.

(12) Bai, Z. P. Ph.D. Thesis, University of Tsukuba, 1991.

Department of Chemistry
University of Tsukuba
Tsukuba, Ibaraki 305, Japan

Takumi Konno*
Ken-ichi Okamoto
Jinsai Hidaka

Received August 30, 1991

An Unusual Species Containing the Mixed-Valence $\{\text{V}^{\text{III}}(\mu\text{-N})\text{V}^{\text{IV}}\}^{4+}$ Core Obtained by Reductive Decomposition of Me_3SiN_3 : $[\text{VBr}_2(\text{N}_3)(\text{dmpe})(\mu\text{-N})\text{VBr}(\text{dmpe})_2]$

One approach to gaining an understanding of nitrogen fixation involves the preparation and study of plausible intermediates in the process, such as nitride complexes. While a reasonably large number of nitride complexes of second- and third-row transition elements have been structurally characterized, there exist by comparison relatively few first-row examples.¹ Recently we have focused some attention on obtaining vanadium nitride complexes from the reaction between low-valent vanadium complexes and azides. Herein are reported the synthesis, structure, and some physical properties of a relatively low-valent asymmetric nitride-bridged divanadium complex, $[\text{VBr}_2(\text{N}_3)(\text{dmpe})(\mu\text{-N})\text{VBr}(\text{dmpe})_2]$ (**1**), which was produced using the aforementioned reaction type under mild conditions. Compound **1** is a trapped mixed-valence $\text{V}^{\text{III}}\text{V}^{\text{IV}}$ complex and is quite distinct from the few high-valent vanadium nitride complexes which have been reported previously.^{2–4}

The vanadium(II) phosphine complex *trans*- $[\text{VBr}_2(\text{dmpe})_2]^{5+}$ (*dmpe* = 1,2-bis(dimethylphosphino)ethane) was generated in solution by mixing 0.250 g (0.443 mmol) of *trans*- $[\text{VBr}_2(\text{tht})_4]^{6+}$ (*tht* = tetrahydrothiophene) and 0.133 g (0.887 mmol) of *dmpe* in 10 mL of tetrahydrofuran (*thf*). After the pink reaction mixture was stirred at room temperature for 1 h, 0.130 g (0.887 mmol) of Me_3SiN_3 was added. Within 1 h a green precipitate⁷ appeared and the solution color had changed to orange. The green precipitate was filtered away and the filtrate was evaporated to dryness. The residue was redissolved in 10 mL of toluene, and 5 mL of hexane were carefully layered on top of the toluene solution. Crystallization was allowed to proceed for 1 week at -35°C . Using this procedure a 34% yield (0.130 g) of compound **1** as red-orange crystals⁸ suitable for X-ray diffraction studies⁹

- (9) Anal. Calcd for $[\text{Co}(\text{NH}_2\text{CH}_2\text{CH}_2\text{SO}_2)_2(\text{NH}_2\text{CH}_2\text{CH}_2\text{NH}_2)]\text{Br}$: C, 17.36; H, 4.86; N, 13.32. Found: C, 17.30; H, 4.94; N, 13.32. Visible–UV spectrum, H_2O solvent [ν_{max} , 10^3 cm^{-1} (log ϵ ; ϵ in $\text{mol}^{-1} \text{ dm}^3 \text{ cm}^{-1}$): 23.20 (2.45), 32.89 (4.17), 34.70 (4.19). NMR (500 MHz, D_2O , ppm from DSS): ^1H NMR δ 2.75 (td, $J = 13$ and 5 Hz, $-\text{CH}_2\text{S}$), 2.90 (br, $-\text{CH}_2\text{N}$ of en), 2.91 (dt, $J = 13$ and 5 Hz, $-\text{CH}_2\text{S}$), 3.00 (br, $-\text{CH}_2\text{N}$ of en), 3.14 (dt, $J = 12$ and 5 Hz, $-\text{CH}_2\text{N}$), and 3.78 (td, $J = 12$ and 5 Hz, $-\text{CH}_2\text{N}$); ^{13}C NMR, δ 40.83 ($-\text{CH}_2\text{N}$), 46.57 and 46.68 ($-\text{CH}_2\text{N}$ of en), and 64.16 ($-\text{CH}_2\text{S}$). The H_2O_2 oxidation of the ($-$) $_{516}^{\text{CD}}$ isomer of **1** gave the optical isomer of **2**, which shows a major negative CD band at 439 nm.
- (10) (a) Yamanari, K.; Takeshita, N.; Shimura, Y. *Bull. Chem. Soc. Jpn.* **1984**, *57*, 2852. (b) Okamoto, K.; Umehara, H.; Hidaka, J. *Bull. Chem. Soc. Jpn.* **1987**, *60*, 2875. (c) Konno, T.; Umehara, H.; Okamoto, K.; Hidaka, J. *Bull. Chem. Soc. Jpn.* **1989**, *62*, 3015.
- (11) Umehara, H. Ph.D. Thesis, University of Tsukuba, 1988.

- (1) Nugent, W. A.; Mayer, J. M. *Metal-Ligand Multiple Bonds*; Wiley: New York, 1988.
- (2) Critchlow, S. C.; Lerchen, M. E.; Smith, R. C.; Doherty, N. M. *J. Am. Chem. Soc.* **1988**, *110*, 8071–8075.
- (3) Willing, W.; Christophersen, R.; Muller, U.; Dehnicke, K. Z. *Anorg. Allg. Chem.* **1987**, *555*, 16–22.
- (4) Goedken, V. L.; Ladd, J. A. *J. Chem. Soc., Chem. Commun.* **1981**, 910–911.
- (5) The dichloride analogue has been described previously: Girolami, G. S.; Wilkinson, G.; Galas, A. M. R.; Thornton-Pett, M.; Hursthouse, M. B. *J. Chem. Soc., Dalton Trans.* **1985**, 1339–1348.
- (6) Sable, D. B.; Wilisch, W. C. A.; Hagen, K. S.; Armstrong, W. H. Submitted for publication.
- (7) This green product has recently been identified as *trans*- $[\text{V}(\text{NSiMe}_3)\text{Br}(\text{dmpe})_2](\text{Br})$ and will be the subject of a future report.
- (8) Satisfactory element analyses (CHN) were obtained for compound **1**.

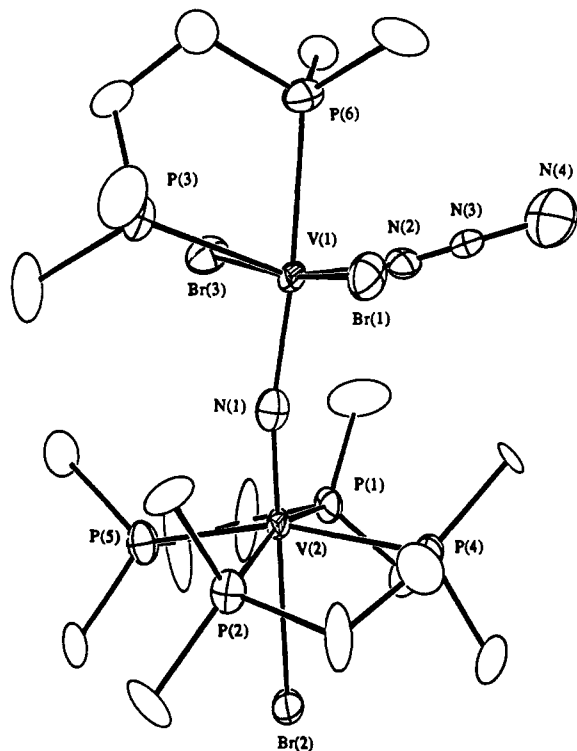


Figure 1. Structure of $[\text{VBr}_2(\text{N}_3)(\text{dmpe})(\mu\text{-N})\text{VBr}(\text{dmpe})_2]$ (**1**) showing the 30% probability thermal ellipsoids and atom-labeling scheme. Hydrogen atoms are omitted for clarity. Selected interatomic distances (\AA) and angles (deg) are as follows: $\text{V}(1)\text{-N}(1) = 1.972$ (14), $\text{V}(1)\text{-Br}(1) = 2.567$ (4), $\text{V}(1)\text{-Br}(3) = 2.589$ (4), $\text{V}(1)\text{-N}(2) = 2.037$ (14), $\text{V}(1)\text{-P}(3) = 2.588$ (7), $\text{V}(1)\text{-P}(6) = 2.586$ (7), $\text{V}(2)\text{-N}(1) = 1.652$ (15), $\text{V}(2)\text{-Br}(2) = 2.739$ (4), $\text{V}(2)\text{-P}(1) = 2.498$ (6), $\text{V}(2)\text{-P}(5) = 2.516$ (7), $\text{V}(2)\text{-P}(2) = 2.481$ (6), $\text{V}(2)\text{-P}(4) = 2.507$ (6), $\text{N}(2)\text{-N}(3) = 1.020$ (19), $\text{N}(3)\text{-N}(4) = 1.250$ (23), $\text{V}(1)\text{-N}(1)\text{-V}(2) = 165.1$ (9), $\text{N}(2)\text{-N}(3)\text{-N}(4) = 173.5$ (18), $\text{V}(1)\text{-N}(2)\text{-N}(3) = 136.3$ (13), $\text{Br}(1)\text{-V}(1)\text{-Br}(3) = 169.37$ (16), $\text{Br}(2)\text{-V}(2)\text{-N}(1) = 178.9$ (5), $\text{P}(6)\text{-V}(1)\text{-N}(1) = 174.3$ (5).

was obtained. It is interesting to note that while the orange product reported here contains both nitride and azide ligands, a related reaction between Cp^*_2V and Me_3SiN_3 afforded only the azide complex $[\text{Cp}^*_2\text{V}(\text{N}_3)]$.¹⁰ Also, it has been shown that the reaction between Cp^*_2V and $\text{C}_6\text{H}_5\text{N}_3$ produces $[\text{Cp}^*_2\text{V}(\text{NC}_6\text{H}_5)]$.¹⁰

The crystal structure of **1**, shown in Figure 1, consists of an asymmetric, nonlinear ($\text{V}(1)\text{-N}(1)\text{-V}(2) = 165.1$ (9) $^\circ$) nitride-bridged binuclear species with the $\text{V}(2)\text{-N}(1)$ distance (1.652 (15) \AA) being consistent with a triple bond¹ and the $\text{V}(1)\text{-N}(1)$ separation (1.972 (14) \AA) being indicative of a single bond. This structure is remarkably distinct from that of the V^{V} species $[\text{V}(\mu\text{-N})\text{Cl}_2(\text{py})_2]_\infty$ ^{2,3} in which the V -nitride distances are 1.571 (7) and 2.729 (7) \AA .² As noted previously for this latter case the nitride bridge is very weak at best.^{2,3} Evidently the nitride group bound to lower valent vanadium atoms in **1** is a much better bridging ligand. The short $\text{V}(2)\text{-N}(1)$ distance as well as somewhat smaller $\text{V}(2)\text{-P}$ separations, as compared to the $\text{V}(1)\text{-P}$ bonds, supports the assignment of $\text{V}(2)$ as the V^{IV} center and $\text{V}(1)$ as the V^{III} ion. The average V-P distance in **1** (2.529 \AA) is slightly longer than the same for $[\text{VCl}_2(\text{dmpe})_2]$ (2.499 \AA).⁵ The strong trans influence of $\text{N}(1)$ gives rise to a rather long $\text{V}(2)\text{-Br}(2)$ bond (2.739 (4) \AA). Nitrogen-nitrogen bond distances in the coord-

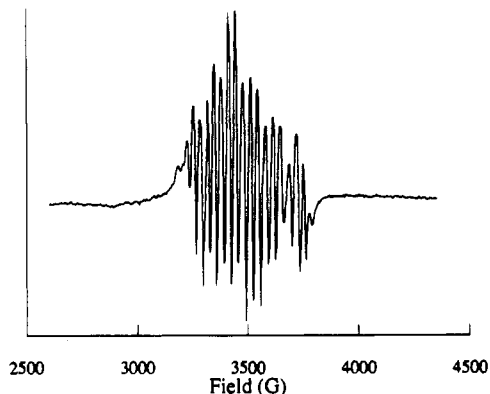


Figure 2. X-Band ($\nu = 9.82$ GHz) EPR spectrum of **1** in tetrahydrofuran at 298 K obtained by using the following instrument settings: microwave power, 12.6 mW; field modulation amplitude, 10 G; modulation frequency, 100 kHz.

inated azide are somewhat unusual in comparison to other metal azide species.¹¹ Generally one would predict that the $\text{N}(2)\text{-N}(3)$ bond should be shorter than the $\text{N}(3)\text{-N}(4)$ bond.¹¹ The opposite is observed for **1** and was also noted for the structure of $[\text{Ni}(\text{P}(\text{C}_6\text{H}_5)_3)_2(\text{NO})(\text{N}_3)]$.^{12a} A crystallographic disorder that could account for the anomalous azide bond distances in both of these cases was discussed by Enemark.^{12a} In our case the proposed origin of the unusual apparent azide geometry would correspond to azide/bromide disorder due to the presence of an impurity of $[\text{VBr}_3(\text{dmpe})(\mu\text{-N})\text{VBr}(\text{dmpe})_2]$ in crystals of **1**. Unusual apparent M-O distances associated with "bond-stretch isomers" have been recently shown to be caused by a similar phenomenon.^{12b}

Compound **1** was characterized using several physical techniques. The electronic absorption spectrum of **1** in THF has maxima at 1189 nm ($\epsilon = 6 \text{ cm}^{-1} \text{ M}^{-1}$) and 802 nm ($\epsilon = 21$) and a shoulder at 477 nm. The lowest energy electronic transition may correspond to an intervalence band. The infrared (IR) spectrum of **1** contains bands for the dmpe ligands which correspond to those observed for $[\text{VCl}_2(\text{dmpe})_2]$.⁵ Absorptions at 278 and 265 cm^{-1} for **1** are attributed to V-Br stretches. The azide asymmetric vibration occurs at 2057 cm^{-1} and can be compared with values for other vanadium azido complexes such as $[\text{Cp}_2\text{V}(\text{N}_3)_2]$ (2069 cm^{-1}),¹³ $[\text{VO}(\text{OPr}^i)(\text{N}_3)_2]$ (2100–2080 cm^{-1}),¹⁴ and $[\text{Cp}^*_2\text{V}(\text{N}_3)]$ (2065 cm^{-1}).¹⁰ An IR band for **1** at 1068 cm^{-1} is assigned to the asymmetric VNV stretch. This value falls within the range observed for other nitride-bridged species (1050–1120 cm^{-1}),¹⁵ and is markedly higher in energy than the corresponding vibration for the V^{V} complex $[\text{V}(\mu\text{-N})\text{Cl}_2(\text{py})_2]_\infty$ (968 cm^{-1}).² The X-band electron paramagnetic resonance (EPR) spectrum for **1** in THF at room temperature displays a 19-line pattern centered at $g = 2$, with an average splitting of 35 G (Figure 2). While a detailed understanding of this pattern will require knowledge of the solution structure of **1** and a theoretical simulation, we hypothesize that the signal is associated principally with the V^{IV} center. Furthermore, it is likely that the EPR spectrum consists of eight principal lines (^{51}V , $I = 7/2$) which are split by the dmpe phosphorous nuclei. The 19-line spectrum observed is consistent with what one would predict for a ratio of hyperfine coupling constants $A_{51\text{V}}/A_{31\text{P}}$ of ~ 2 , assuming that the four phosphorous atoms are effectively equivalent.¹⁶

In conclusion, an interesting nitride-bridged divanadium complex was synthesized using reductive decomposition of Me_3SiN_3 by a V^{II} precursor. The crystal structure of the product confirms

(9) Crystal data for compound $1\cdot 2\text{CH}_2\text{Cl}_2$: orthorhombic space group $Pbca$, $a = 12.421$ (5) \AA , $b = 28.339$ (11) \AA , $c = 26.264$ (6) \AA , $V = 9245$ (10) \AA^3 , $D_c = 1.48 \text{ g cm}^{-3}$, $Z = 8$. Data were collected at 188 K with $\text{Mo K}\alpha$ radiation out to $2\theta = 45^\circ$, yielding 2244 reflections with $I > 3\sigma(I)$. The structure was solved by the G. Sheldrick program SHELXS86 and refined using anisotropic thermal parameters for all non-hydrogen atoms, except C(4) and the two disordered solvent molecules (total of 381 parameters), to R (R_w) values of 6.28% (6.31%).

(10) Osborne, J. H.; Rheingold, A. L.; Troglor, W. C. *J. Am. Chem. Soc.* **1985**, *107*, 7945–7952.

(11) Dori, Z.; Ziolo, R. F. *Chem. Rev.* **1973**, *73*, 247–254.

(12) (a) Enemark, J. H. *Inorg. Chem.* **1971**, *10*, 1952–1957. (b) Yoon, K.; Parkin, G.; Rheingold, A. L.; *J. Am. Chem. Soc.* **1991**, *113*, 1437–1438.

(13) Moran, M.; Gayoso, M. *J. Organomet. Chem.* **1983**, *243*, 423–426.

(14) Choukroun, R.; Gervais, D. *J. Chem. Soc., Dalton Trans.* **1980**, 1800–1802.

(15) Nakamoto, K. *Infrared and Raman Spectra of Inorganic and Coordination Compounds*; Wiley: New York, 1986; p 323.

(16) A similar multiline ESR signal has been observed for $[\text{V}(\text{NSiMe}_3)\text{Br}(\text{dmpe})_2]\text{Br}$.

the core oxidation state assignment $\{V^{III}(\mu-N)V^{IV}\}^{4+}$. Ongoing studies are directed toward exploring the magnetic properties, reactivity of the nitride group and substitution of the nonbridging ligands in 1.

Acknowledgment. Funding for this work was provided by the National Science Foundation (Grant No. CHE-8857455).

Supplementary Material Available: A fully labeled ORTEP drawing and tables of crystallographic data, positional and isotropic thermal param-

eters, anisotropic thermal parameters, interatomic distances, and interatomic angles (9 pages); a table of structure factors (64 pages). Ordering information is given on any current masthead page.

Department of Chemistry
University of California
Berkeley, California 94720

David B. Sable
William H. Armstrong*

Received June 11, 1991

Articles

Contribution from the Institute of Physical Chemistry,
NCSR Demokritos, 153-10 Athens, Greece

Photocatalytic Oxidation of Organic Compounds by Polyoxometalates of Molybdenum and Tungsten. Catalyst Regeneration by Dioxygen

A. Hiskia and E. Papaconstantinou*

Received July 24, 1991

Catalyst regeneration (reoxidation) is key to the effective photocatalytic oxidation of a variety of organic compounds by polyoxometalates. This paper reports on the reoxidation mechanism of photoreduced polyoxometalates by dioxygen. The overall general reaction, presented generally as $M^{(n+1)-} + 1/4 O_2 + H^+ \rightarrow M^{n-} + 1/2 H_2O$ [where $M^{n-} = P_2W_{18}O_{62}^{6-}$ ($P_2W_{18}^{6-}$), $SiW_{12}O_{40}^{4-}$ (SiW_{12}^{4-}), $H_2W_{12}O_{40}^{6-}$ ($H_2W_{12}^{6-}$)], appears to be first order with respect to polyoxometalates and oxygen and zero order with respect to H^+ at $pH < 1.5$ and $pH > 3$. At the inflection point, the order with respect to H^+ , is 1.1 ± 0.4 . Rate constants at low pH are 3.8×10^{-3} , 1.0, and $> 5.5 s^{-1}$ and at high pH are 0.0, 2.7×10^{-2} , and $0.15 s^{-1}$ for $P_2W_{18}^{7-}$, SiW_{12}^{5-} , and $H_2W_{12}^{7-}$, respectively (Figure 3). Reoxidation of molybdates is known to be considerably slower; $P_2Mo_{18}^{8-}$ is not reoxidized by dioxygen, whereas $P_2Mo_{18}^{10-}$ reoxidation is from 4 to more than 6 times slower than that of the polyoxotungstates in acid solution. As previously shown with the molybdates, the rates are a function of the degree of reduction; for instance, the rate constants for doubly reduced $P_2W_{18}^{8-}$ are about 5 times larger than those for the corresponding singly reduced $P_2W_{18}^{7-}$ anions under identical conditions. The rates parallel the redox potential of the polyoxometalates. Limited work was also done with hydrogen peroxide, which seems to behave differently from dioxygen; the results are compared.

Introduction

There has been considerable growth in understanding the catalytic action of polyoxometalates in the last 10 years.¹ Important industrial applications such as oxidation of unsaturated aldehydes or methacrolein or the hydration of propene or isobutene etc. use polyoxometalates as catalysts.²

The photocatalytic action of these compounds has been demonstrated for the oxidation of a variety of organic compounds. It has been shown that polyoxometalates undergo multielectron photoreduction in the near-visible and UV regions, in the presence of a variety of organic compounds, with concomitant oxidation of the organic compound. Quantum yields of 10-20% have been obtained for the oxidation of alcohols,^{3a} whereas smaller quantum yields have been obtained for other organic compounds,^{3b} Hill and Renneke, though, have reported 100% quantum yields for photoreduction of $W_{10}O_{32}^{4-}$ in the presence of cyclooctane in acid solution.^{3c}

Recently, polyoxometalates have been used in the sensitization of semiconductors⁴ and sensitization of electrodes⁵ and have been claimed to functionalize alkanes photochemically.^{3c,6}

Polyoxometalates participate in catalytic processes as "oxygen relays" and/or as electron relays. The first case, in broad terms, represents, primarily, heterogeneous reactions. For instance, it has been shown that the oxidation of CO to CO₂ involves oxygen from the polyoxometalate which is, subsequently, replenished by atmospheric oxygen.² In homogeneous catalytic processes, including photocatalysis, polyoxometalates serve, primarily, as electron relays in electron-transfer and/or hydrogen-transfer reactions.

Key to their acting as homogeneous redox catalysts is the ability of polyoxometalates to accept and release a certain number of electrons without decomposition. An important step in the photocatalytic cycle is the regeneration (reoxidation) of catalyst. Whereas, generally speaking, molybdates are better oxidizing reagents than tungstates, their reoxidation by dioxygen is very slow; many times, reoxidation requires the use of activated carbon with dioxygen or the use of hydrogen peroxide.² On the other hand, tungstates are difficult to reduce, yet their reoxidation by dioxygen is fast and effective.

Apart from generalities, such as reduced tungstates reoxidizing faster than molybdates and some rate constants being obtained with laser flash photolysis techniques,^{7,8c} no systematic study for the reoxidation of polyoxometalates by dioxygen has been reported. Studies of the reoxidation of mixed molybdovanadates by dioxygen by Matveev et al. present an overall complicated picture that is rather different from the reoxidation of simple polyoxometalates discussed in this paper.^{2b}

- (1) Pope, M. T. *Heteropoly and Isopoly Oxometalates*; Springer-Verlag: Berlin, 1983.
- (2) (a) Misono, M. *Catal. Rev.—Sci. Eng.* **1987**, *29*, 269. (b) Kozhevnikov, I. V.; Matveev, K. I. *Russ. Chem. Rev. (Engl. Transl.)* **1982**, *51*, 11. (c) Kozhevnikov, I. V. *Russ. Chem. Rev. (Engl. Transl.)* **1987**, *56*, 811.
- (3) (a) Hiskia, A.; Papaconstantinou, E. *Polyhedron* **1988**, *7*, 477. (b) Dimotikali, D.; Papaconstantinou, E. *Inorg. Chim. Acta* **1984**, *87*, 177. (c) Renneke, R. F.; Hill, C. L. *Angew. Chem., Int. Ed. Engl.* **1988**, *27*, 1526.
- (4) Kiwi, J.; Gratzel, M. *J. Phys. Chem.* **1987**, *91*, 6673.
- (5) Keita, B.; Nadjo, L. *J. Electroanal. Chem. Interfacial Electrochem.* **1988**, *243*, 87.
- (6) (a) Renneke, R. F.; Hill, C. L. *J. Am. Chem. Soc.* **1986**, *108*, 3528. (b) Muradov, M. Z.; Rustamov, M. I. *Dokl. Chem. (Engl. Transl.)* **1988**, *303*, 1051. (c) Zakrzewski, J.; Chauveau, F.; Giannotti, C. *Abstracts, Joint Meeting of the Italian and French Photochemistry Groups, La Baume-les-Aix, France, Oct 1989*; p 36.

- (7) Papaconstantinou, E. *J. Chem. Soc., Chem. Commun.* **1982**, 12.
- (8) (a) Saidkhanov, S. S.; Kokorin, A. I.; Savinov, E. N.; Vokov, A. I.; Parmon, V. N. *J. Mol. Catal.* **1983**, *31*, 365. (b) Ioannidis, A.; Papaconstantinou, E. *Inorg. Chem.* **1985**, *24*, 349. (c) Akid, R.; Darwent, J. R. *J. Chem. Soc., Dalton Trans.* **1985**, 395. (d) Yamase, T. *Inorg. Chim. Acta* **1982**, *64*, L155. (e) Hill, C. L.; Bouchard, D. A. *J. Am. Chem. Soc.* **1985**, *107*, 5148. (f) Fox, M. A.; Cordona, R.; Gailard, E. *Ibid.* **1987**, *109*, 6347.